

Bergische Universität Wuppertal

Fakultät für Mathematik und Naturwissenschaften

Institute of Mathematical Modelling, Analysis and Computational Mathematics (IMACM)

Preprint BUW-IMACM 26/25

Himanshu Kumar Dwivedi and Matthias Ehrhardt

Mass-lumped finite elements with maximum-bound preservation and original-energy dissipation for the degenerate-mobility Allen-Cahn equation

November 6, 2026

http://www.imacm.uni-wuppertal.de

Mass-lumped finite elements with maximum-bound preservation and original-energy dissipation for the degenerate-mobility Allen-Cahn equation

Himanshu Kumar Dwivedi[a], Matthias Ehrhardt[b,*]

[a]Department of Mathematical Sciences, Indian Institute of Technology (BHU), Varanasi-221005, India.
[b]Applied and Computational Mathematics, University of Wuppertal, Gaußstraße 20, 42119 Wuppertal, Germany

ARTICLE INFO

Keywords:
Allen-Cahn equation
degenerate mobility
mass-lumped finite element method
maximum-bound principle
energy dissipation

ABSTRACT

In this work, we propose a mass-lumped finite element method for the Allen-Cahn equation that incorporates nonlinear mobility which may degenerate. The spatial approximation uses continuous, piecewise linear, mass-lumped finite elements, while convex splitting is employed for the double-well potential in time. Under the standard non-obtuse mesh condition, it is shown that the resulting fully discrete method preserves the maximum-bound principle unconditionally: if the initial approximation takes values in $[-1, 1]$, then so does the numerical solution at every time level. Additionally, the method dissipates the original discrete Ginzburg-Landau energy without any time-step restriction, even when the mobility vanishes at pure phases. This analysis relies on the monotonicity of the lumped finite element operator and the convexity of the split potential. Numerical experiments confirm these theoretical properties and demonstrate the robustness of the method in phase-separation dynamics involving degenerate mobility.

1. Introduction

The Allen-Cahn equation is a fundamental phase-field model used to describe interfacial dynamics and phase separation. It was originally introduced to describe antiphase boundary motion in crystalline solids [1]. A classic numerical analysis of the model and its relation to mean-curvature flow can be found in [5]. In many applications, the relaxation rate depends on the local phase state and is therefore modeled through as a nonlinear mobility. In this paper, we investigate the *generalized Allen-Cahn model* described by the following system:

$$\begin{cases} \frac{\partial u}{\partial t} = -M(u)\mu, \qquad \mu = -\varepsilon^2 \Delta u + f(u), & (\mathbf{x}, t) \in \Omega \times (0, T], \\ \frac{\partial u}{\partial \mathbf{n}} = 0, & (\mathbf{x}, t) \in \partial\Omega \times (0, T], \\ u(\mathbf{x}, 0) = u_0(\mathbf{x}), & \mathbf{x} \in \Omega. \end{cases} \tag{1}$$

Here, $\Omega \subset \mathbb{R}^d$ $(d = 2, 3)$ is a bounded polygonal or polyhedral domain, $\mathbf{n}$ represents the outward-pointing unit normal vector, and $\varepsilon > 0$ is the interfacial width. Hereafter, $(\cdot, \cdot)$ and $\|\cdot\|_0$ denote the $L^2(\Omega)$ inner product and norm, respectively. Moreover,

$$F(u) = \frac{(u^2 - 1)^2}{4}, \quad \text{is the bistable potential with } \; f(u) = F'(u) = u^3 - u.$$

The mobility $M(u)$ is assumed to be nonnegative for $u \in [-1, 1]$ and is allowed to degenerate at the pure phases. One example is $M(u) = (1 - u^2)^m$, where m is a positive integer. The considered model has two important structural properties. If $\|u_0\|_{L^\infty(\Omega)} \leq 1$, the solution remains bounded by the pure phases, while the *Ginzburg-Landau energy*

$$E(u) = \int_\Omega \left(\frac{\varepsilon^2}{2} |\nabla u|^2 + F(u) \right) d\mathbf{x} \tag{2}$$

*Corresponding author
himanshukrdwivedi.rs.mat21@itbhu.ac.in (H.K. Dwivedi); ehrhardt@uni-wuppertal.de (M. Ehrhardt)
ORCID(s): 0000-0002-2829-8764 (H.K. Dwivedi); 0000-0003-2561-8854 (M. Ehrhardt)

formally satisfies

$$\frac{dE}{dt} = -\big(M(u)\mu, \mu\big) \le 0.$$

Maintaining both properties at the discrete level is even more crucial when M is degenerate because violating the maximum-bound can easily cause the mobility to become negative and lose its physical interpretation.

Considerable work has been devoted to structure-preserving discretizations of Allen-Cahn-type equations. For nonlinear and possibly degenerate mobility, Shen, Tang and Yang [12] constructed maximum-principle-preserving finite-difference (FD) schemes for the generalized Allen-Cahn equation. Meanwhile, Du and Hou [3] developed a second-order, maximum-bound-preserving FD method for a generalized model with nonlinear mobility and convection. Second-order BDF and stabilized Crank-Nicolson schemes for general mobility were subsequently analyzed in [7]. More recently, Hou, Liu and Ju [9] obtained a second-order FD method that simultaneously preserves the maximum-bound principle and dissipates the original energy. Hou, Zhang and Zhu [8] developed an unconditionally maximum-bound-preserving second-order scheme. Fu et al. [6] addressed degenerate mobilities through dynamic stabilization. Their first-order method unconditionally preserves both the maximum-bound principle and energy dissipation, while the second-order formulation satisfies a conditional maximum-bound principle and a uniform original energy bound.

The finite element method (FEM) provides greater geometric flexibility, but preserving these structures simultaneously is more challenging. Barrett and Blowey [2] developed an early finite element analysis for degenerate Allen-Cahn/Cahn-Hilliard systems. For the classical Allen-Cahn equation, energy-stable FEMs have been studied in [11]. Mass-lumped, maximum-principle-preserving formulations have also been developed for surface Allen-Cahn equations [13]. Subsequently, Yang, Yi, and Zhang [14] proposed high-order mass-lumped FEM schemes that unconditionally preserve the maximum principle for the classical Allen-Cahn equation. However, FEM theory for nonlinear mobility, which can vanish at pure phases, is comparatively underdeveloped. This is especially true when a rigorous nodal maximum-bound and dissipation of the original Ginzburg-Landau energy are both required within the same fully discrete formulation.

Motivated by this observation, we construct a mass-lumped P_1 finite element scheme for (1) in conjunction with convex-splitting for the double-well potential. The diagonal property of mass lumping, combined with the sign structure of the stiffness matrix on non-obtuse simplicial meshes, enables us to establish a maximum-bound principle for the scheme using a direct nodal argument. Meanwhile, the convex splitting results in the original discrete energy law. We prove that, for arbitrary time step sizes, the method satisfies

$$|U_h^n|_{L^\infty(\Omega)} \le 1, \quad \text{and} \quad E_h(U_h^n) \le E_h(U_h^{n-1}), \quad \text{provided} \quad \|U_h^0\|_{L^\infty(\Omega)} \le 1.$$

In particular, the analysis remains valid when $M(\pm 1) = 0$. We conducted numerical experiments to assess the accuracy of the proposed scheme, confirming that it maintains both the maximum-bound principle and the energy-dissipation property.

2. Mass-lumped finite element approximation

Let $\mathcal{T}_h$ be a conforming and shape-regular simplicial partition of Ω, consisting of triangles for $d = 2$ and tetrahedra for $d = 3$, and let $h = \max_{K\in\mathcal{T}_h} \operatorname{diam}(K)$. We consider the continuous piecewise linear finite element space

$$V_h = \big\{ v_h \in C(\overline{\Omega}) : \ v_h|_K \in \mathbb{P}_1(K) \quad \forall\, K \in \mathcal{T}_h \big\}.$$

We denote by $\{x_i\}_{i=1}^{N_h}$ the vertices of $\mathcal{T}_h$ and by $\{\phi_i\}_{i=1}^{N_h}$ the corresponding nodal basis satisfying $\phi_i(x_j) = \delta_{ij}$. For any nodal functions v and w, we introduce the *mass-lumped inner product*

$$(v, w)_h := \sum_{i=1}^{N_h} v(x_i)\, w(x_i)\, m_i, \quad \text{where} \quad m_i := \int_\Omega \phi_i(\mathbf{x})\, d\mathbf{x} > 0, \tag{3}$$

and introduce the induced norm $\|v_h\|_h^2 = (v_h, v_h)_h$. Thus, the associated mass matrix is diagonal with strictly positive diagonal entries. We recall that we also use the standard inner product (without the subscript h). Mass lumping is particularly useful in maximum-principle analysis since it preserves the nodal character of the discrete evolution [10, 14].

For the stiffness matrix $A = (a_{ij})_{i,j=1}^{N_h}$, let $a_{ij} := (\nabla\phi_j, \nabla\phi_i)$. Throughout the analysis, we impose the standard non-obtuse mesh condition

$$a_{ij} \le 0, \qquad i \ne j. \tag{4}$$

This condition (4) ensures that the finite element stiffness matrix A possesses the monotonicity structure required by a discrete maximum principle [10]. Since the nodal basis forms a partition of unity and no essential boundary degrees of freedom are eliminated under the homogeneous Neumann condition, we have

$$\sum_{j=1}^{N_h} a_{ij} = 0, \qquad 1 \le i \le N_h. \tag{5}$$

To obtain an *energy-stable temporal approximation*, we use a convex splitting of the double-well potential

$$F(s) = F_c(s) - F_e(s), \quad \text{with} \qquad F_c(s) = \tfrac{1}{4}s^4 + \tfrac{1}{4}, \qquad F_e(s) = \tfrac{1}{2}s^2, \tag{6}$$

where both F_c and F_e are convex. Consequently, $F_c'(s) = s^3$, and $F_e'(s) = s$. This decomposition enables us to treat the convex contribution implicitly and the concave contribution explicitly. This is the key mechanism behind the discrete energy law [4, 11].

Next, let $0 = t_0 < t_1 < \cdots < t_N = T$ be a uniform temporal partition with time step $\tau = T/N$, and define

$$\delta_\tau U_h^{n+1} := \frac{U_h^{n+1} - U_h^n}{\tau}.$$

Assuming $u_0 \in C(\overline{\Omega})$, we set $U_h^0 = I_h u_0$, where I_h denotes the nodal interpolation operator. Given $U_h^n \in V_h$, the proposed mass-lumped FEM seeks to find $(U_h^{n+1}, \mu_h^{n+1}) \in V_h \times V_h$ such that, for all $v_h, q_h \in V_h$,

$$\left(\delta_\tau U_h^{n+1}, v_h\right)_h + \left(M(U_h^n)\mu_h^{n+1}, v_h\right)_h = 0, \tag{7a}$$

$$\left(\mu_h^{n+1}, q_h\right)_h = \varepsilon^2\left(\nabla U_h^{n+1}, \nabla q_h\right) + \left((U_h^{n+1})^3 - U_h^n, q_h\right)_h. \tag{7b}$$

Here and below, nonlinear quantities appearing in $(\cdot,\cdot)_h$ are evaluated nodally. In particular, $M_i^n := M\left(U_h^n(x_i)\right)$. No strictly positive lower bound on the mobility is imposed. We only require

$$M(s) \ge 0, \qquad s \in [-1, 1], \tag{8}$$

so that genuinely degenerate mobilities, such as

$$M(s) = (1 - s^2)^m, \qquad m \in \mathbb{N},$$

are included. Notice that if $M_i^n = 0$, then equation (7a) simply implies $U_h^{n+1}(x_i) = U_h^n(x_i)$ at the corresponding node. Therefore, the discrete formulation remains well-defined at pure phases.

For later use, we record the nodal representation of (7). Choosing $v_h = q_h = \phi_i$ yields the following system:

$$m_i \frac{U_i^{n+1} - U_i^n}{\tau} + m_i M_i^n \mu_i^{n+1} = 0, \tag{9a}$$

$$m_i \mu_i^{n+1} = \varepsilon^2 \sum_{j=1}^{N_h} a_{ij} U_j^{n+1} + m_i\left[(U_i^{n+1})^3 - U_i^n\right], \tag{9b}$$

where $U_i^n := U_h^n(x_i)$, and $\mu_i^n := \mu_h^n(x_i)$. Eliminating μ_i^{n+1} from (9), we obtain

$$U_i^{n+1} + \tau M_i^n \left[\frac{\varepsilon^2}{m_i} \sum_{j=1}^{N_h} a_{ij}\, U_j^{n+1} + (U_i^{n+1})^3\right] = (1 + \tau M_i^n)\, U_i^n. \tag{10}$$

Together with (4)–(5), the representation (10) will provide a direct nodal mechanism for establishing the maximum-bound principle.

Finally, corresponding to the Ginzburg-Landau energy in (2), we define the *mass-lumped discrete energy*

$$E_h(V_h) := \frac{\varepsilon^2}{2}\|\nabla V_h\|_0^2 + \big(F(V_h),1\big)_h = \frac{\varepsilon^2}{2}\|\nabla V_h\|_0^2 + \sum_{i=1}^{N_h} m_i F(V_h(x_i)). \tag{11}$$

The combination of the diagonal lumped mass matrix and the stiffness-matrix sign structure yields the discrete maximum-bound. Meanwhile, the convex splitting in (7b) leads directly to dissipation of the original energy (11). These two essential properties are established in the next section.

3. Maximum-bound and energy-dissipation properties

We will now establish the two main structural properties of the scheme (7). Throughout this section, we will assume that the mesh condition (4) and the mobility assumption (8) hold.

3.1. Well-posedness

Suppose that $M_i^n := M(U_i^n) \geq 0$ for all i. If $M_i^n = 0$, then (9a) immediately yields $U_i^{n+1} = U_i^n$. On the remaining set $\mathcal{I}_+^n := \{i : M_i^n > 0\}$, eliminating μ_i^{n+1} from (9) gives

$$\frac{m_i}{\tau M_i^n}(U_i^{n+1} - U_i^n) + \varepsilon^2 \sum_{j=1}^{N_h} a_{ij} U_j^{n+1} + m_i\big[(U_i^{n+1})^3 - U_i^n\big] = 0. \tag{12}$$

The system (12) is the Euler equation of the functional

$$\mathcal{J}_n(V_h) = \sum_{i\in\mathcal{I}_+^n} \frac{m_i}{2\tau M_i^n}(V_i - U_i^n)^2 + \frac{\varepsilon^2}{2}\|\nabla V_h\|_0^2 + \sum_{i\in\mathcal{I}_+^n} m_i\Big(\frac{1}{4}V_i^4 - U_i^n V_i\Big), \tag{13}$$

defined on the affine subspace satisfying $V_i = U_i^n$ for $i \notin \mathcal{I}_+^n$. Since the first term in (13) is strictly convex on the active nodes and the remaining quadratic and quartic terms are convex, $\mathcal{J}_n$ is coercive and strictly convex. Therefore, it admits a unique minimizer. The chemical potential is subsequently uniquely determined from (9b). Therefore, the fully discrete problem is well-posed.

3.2. Maximum-bound analysis

The following elementary property of the stiffness operator is central to the maximum-bound analysis.

Lemma 3.1. *Let $V_h = \sum_{j=1}^{N_h} V_j\phi_j \in V_h$ and assume (4)-(5). If $V_i = \max_j V_j$, then $\sum_{j=1}^{N_h} a_{ij}V_j \geq 0$. If $V_i = \min_j V_j$, then $\sum_{j=1}^{N_h} a_{ij}V_j \leq 0$.*

Proof. Using (5), we have

$$\sum_{j=1}^{N_h} a_{ij}V_j = \sum_{j\neq i} a_{ij}(V_j - V_i).$$

Since $a_{ij} \leq 0$ for $j \neq i$, and at a nodal maximum, $V_j - V_i \leq 0$, the first assertion is proven. The argument at a nodal minimum is identical, but with the inequalities reversed. □

We are now ready to establish the *discrete maximum-bound principle*.

Theorem 3.2 (maximum-bound principle)**.** *Assume that $\|U_h^0\|_{L^\infty(\Omega)} \leq 1$, and that $M(s) \geq 0$ for $s \in [-1,1]$. Then, for arbitrary $\tau > 0$, the solution of (7) satisfies*

$$\|U_h^n\|_{L^\infty(\Omega)} \leq 1, \qquad 0 \leq n \leq N. \tag{14}$$

Proof. We proceed by induction. The assertion is true for $n = 0$. Suppose that $|U_i^n| \le 1$ for all nodes x_i. By (8), we have $M_i^n = M(U_i^n) \ge 0$. Assume, to the contrary, that

$$U_{i_*}^{n+1} = \max_{1\le i\le N_h} U_i^{n+1} > 1.$$

By Lemma 3.1,

$$\sum_{j=1}^{N_h} a_{i_* j}\, U_j^{n+1} \ge 0.$$

Hence, from the nodal equation (10),

$$(1+\tau M_{i_*}^n)\, U_{i_*}^n = U_{i_*}^{n+1} + \tau M_{i_*}^n \left[\frac{\varepsilon^2}{m_{i_*}} \sum_{j=1}^{N_h} a_{i_* j}\, U_j^{n+1} + (U_{i_*}^{n+1})^3\right] \ge U_{i_*}^{n+1} + \tau M_{i_*}^n\, (U_{i_*}^{n+1})^3 > 1 + \tau M_{i_*}^n.$$

On the other hand, the induction hypothesis gives

$$(1+\tau M_{i_*}^n)\, U_{i_*}^n \le 1 + \tau M_{i_*}^n,$$

which is a contradiction. Therefore, $\max_i U_i^{n+1} \le 1$. Similarly, suppose that

$$U_{i_*}^{n+1} = \min_{1\le i\le N_h} U_i^{n+1} < -1.$$

From Lemma 3.1 we get the following

$$\sum_{j=1}^{N_h} a_{i_* j}\, U_j^{n+1} \le 0.$$

Using (10), we obtain

$$(1+\tau M_{i_*}^n)\, U_{i_*}^n \le U_{i_*}^{n+1} + \tau M_{i_*}^n (U_{i_*}^{n+1})^3 < -1 - \tau M_{i_*}^n,$$

whereas the induction hypothesis yields

$$(1+\tau M_{i_*}^n)\, U_{i_*}^n \ge -1 - \tau M_{i_*}^n.$$

This is again a contradiction. Thus $-1 \le U_i^{n+1} \le 1$ at every node. Since U_h^{n+1} is piecewise linear, its extrema on every simplex are attained at the vertices, and hence (14) follows. The induction is complete. □

A consequence of Theorem 3.2 is that $M(U_h^n) \ge 0$ at every time level, including the degenerate case $M(\pm 1) = 0$.

3.3. Energy-dissipation properties

We next show that the same scheme dissipates the original discrete Ginzburg-Landau energy (11).

Theorem 3.3 (Original-energy dissipation)**.** *Under the assumptions of Theorem 3.2, the solution of* (7) *satisfies the discrete energy identity*

$$E_h(U_h^{n+1}) - E_h(U_h^n) = -\tau\big(M(U_h^n)\mu_h^{n+1}, \mu_h^{n+1}\big)_h - \frac{\varepsilon^2}{2}\|\nabla(U_h^{n+1} - U_h^n)\|_0^2 - \mathcal{R}_h^{n+1}, \tag{15}$$

where

$$\mathcal{R}_h^{n+1} := \frac{1}{4}\sum_{i=1}^{N_h} m_i (U_i^{n+1} - U_i^n)^2 \Big[3(U_i^{n+1})^2 + 2U_i^{n+1}U_i^n + (U_i^n)^2 + 2\Big] \ge 0. \tag{16}$$

Consequently, for every $\tau > 0$, we have the discrete energy decay

$$E_h(U_h^{n+1}) \le E_h(U_h^n), \qquad 0 \le n \le N-1. \tag{17}$$

Proof. First, we set $\delta U_h^{n+1} := U_h^{n+1} - U_h^n$. Taking $v_h = \mu_h^{n+1}$ in (7a) and multiplying by τ gives

$$\left(\delta U_h^{n+1}, \mu_h^{n+1}\right)_h + \tau\left(M(U_h^n)\mu_h^{n+1}, \mu_h^{n+1}\right)_h = 0. \tag{18}$$

Taking $q_h = \delta U_h^{n+1}$ in (7b), we obtain

$$\left(\mu_h^{n+1}, \delta U_h^{n+1}\right)_h = \varepsilon^2\left(\nabla U_h^{n+1}, \nabla \delta U_h^{n+1}\right) + \left((U_h^{n+1})^3 - U_h^n, \delta U_h^{n+1}\right)_h. \tag{19}$$

The gradient contribution satisfies the exact identity

$$\left(\nabla U_h^{n+1}, \nabla \delta U_h^{n+1}\right) = \frac{1}{2}\left(\|\nabla U_h^{n+1}\|_0^2 - \|\nabla U_h^n\|_0^2 + \|\nabla \delta U_h^{n+1}\|_0^2\right). \tag{20}$$

Moreover, for arbitrary $a, b \in \mathbb{R}$ and $F(s) = \frac{1}{4}(s^2-1)^2$, it is straightforward that

$$(a^3 - b)(a - b) = F(a) - F(b) + \frac{(a-b)^2}{4}\left(3a^2 + 2ab + b^2 + 2\right). \tag{21}$$

Since

$$3a^2 + 2ab + b^2 + 2 = 2a^2 + (a+b)^2 + 2 > 0,$$

the last term in (21) is nonnegative. Applying (21) nodewise in the lumped inner product gives

$$\left((U_h^{n+1})^3 - U_h^n, \delta U_h^{n+1}\right)_h = \left(F(U_h^{n+1}) - F(U_h^n), 1\right)_h + \mathcal{R}_h^{n+1}. \tag{22}$$

Substitution of (20) and (22) into (19), followed by (18), yields (15). Finally, Theorem 3.2 ensures $M(U_i^n) \geq 0$ for every node, and therefore

$$\left(M(U_h^n)\mu_h^{n+1}, \mu_h^{n+1}\right)_h = \sum_{i=1}^{N_h} m_i M(U_i^n)(\mu_i^{n+1})^2 \geq 0.$$

Then, the claimed energy dissipation property follows, along with (16), which implies (17). □

Thus, the proposed mass-lumped FEM preserves the intrinsic structures of the degenerate-mobility Allen-Cahn dynamics without any restriction on the time-step size. In particular, the maximum-bound keeps the numerical solution within the physically admissible interval $[-1, 1]$, while (15) shows that the original discrete Ginzburg-Landau energy, rather than a modified one, is dissipated at every time step.

4. Numerical experiments

In this section, we present two numerical examples that demonstrate the accuracy and structure-preserving properties of the proposed method. The computational domain is triangulated by dividing each uniform rectangular cell into two right triangles. Thus, the resulting mesh satisfies the non-obtuse condition (4). All nonlinear systems are solved by Newton iteration using U_h^n as the initial guess. The iterative procedure stops once the relative residual decreases below the prescribed tolerance of 10^{-10}. Unless otherwise stated, we use the degenerate mobility $M(u) = 1 - u^2$.

Example 1. (Accuracy test) First, we consider the forced problem

$$u_t = -M(u)\mu + g(\mathbf{x}, t), \qquad \text{with} \qquad \mu = -\varepsilon^2\Delta u + u^3 - u, \tag{23}$$

on $\Omega = (0,1)^2$, supplemented with homogeneous Neumann boundary conditions. The source term is chosen such that

$$u(\mathbf{x}, t) = \frac{e^{-t}\cos(\pi x)\cos(\pi y)}{2} \tag{24}$$

is the exact solution. In particular, since $\Delta u = -2\pi^2 u$, we take

$$g = -u + (1 - u^2)(2\varepsilon^2\pi^2 u + u^3 - u). \tag{25}$$

Table 1
Numerical errors and convergence rates for Example 1 with $\tau = h^2$.

		L^2-error		H^1-seminorm error	
h	τ	$\|u(T) - U_h^N\|_0$	Rate	$\|\nabla(u(T) - U_h^N)\|_0$	Rate
1/8	1.5625×10^{-2}	3.36204×10^{-3}	-	8.36695×10^{-2}	-
1/16	3.9062×10^{-3}	8.69831×10^{-4}	1.951	4.05445×10^{-2}	1.045
1/32	9.7656×10^{-4}	2.19438×10^{-4}	1.987	2.01082×10^{-2}	1.012
1/64	2.4414×10^{-4}	5.49916×10^{-5}	1.997	1.00347×10^{-2}	1.003

The exact solution satisfies the homogeneous Neumann condition and remains strictly within the admissible interval $[-1, 1]$. We set $\varepsilon = 0.1$, $T = 1$, and choose $\tau = h^2$ so that the first-order temporal error does not dominate the spatial discretization error. At the final time, we measure

$$e_0 = \|u(\cdot, T) - U_h^N\|_0, \qquad e_1 = \|\nabla(u(\cdot, T) - U_h^N)\|_0.$$

The corresponding convergence rates are computed by

$$\text{Rate} = \log_2\Big(\frac{e(h)}{e(h/2)}\Big).$$

The numerical errors are reported in Table 1. as expected, the results exhibit the expected second-order convergence in the L^2 norm and first-order convergence in the H^1 seminorm for the piecewise linear finite element approximation.

Example 2. (Phase separation with degenerate mobility) Next, we examine the long-time phase evolution of the unforced Allen-Cahn problem (1) on $\Omega = (0, 1)^2$. We set $\varepsilon = 0.02$ with $M(u) = 1 - u^2$ and initialize the nodal values with a small random perturbation $U_h^0(x_i) = 0.05\,\xi_i$, where $\xi_i \sim \mathcal{U}[-1, 1]$. Hence,

$$\|U_h^0\|_{L^\infty} \le 0.05 < 1.$$

The computation is performed up to time $T = 10$ on a uniform triangulation with $h = 1/128$ and time step $\tau = 10^{-2}$. To examine the two structural properties established in Theorems 3.2 and 3.3, we monitor the following:

$$U_{\max}^n := \max_{1 \le i \le N_h} U_i^n, \qquad U_{\min}^n := \min_{1 \le i \le N_h} U_i^n, \qquad \mathcal{E}^n := E_h(U_h^n). \tag{26}$$

Representative phase-field configurations, along with the histories of $U_{\max}^n$, $U_{\min}^n$, and $\mathcal{E}^n$ are displayed in Figure 1. The nodal extrema remain in the admissible interval, $-1 \le U_{\min}^n \le U_{\max}^n \le 1$, while the original discrete Ginzburg-Landau energy decreases monotonically, $\mathcal{E}^{n+1} \le \mathcal{E}^n$, in agreement with the theoretical results. Furthermore, the mobility $M(u) = 1 - u^2$ decreases as $|u|$ approaches one and vanishes at the pure phases. This illustrates the effect of mobility degeneracy on the interfacial evolution.

5. Conclusion

We have developed a mass-lumped P_1 FEM for the Allen-Cahn problem involving nonlinear, potentially degenerate mobility. Combining mass lumping with a convex-splitting treatment of the double-well potential preserves the nodal maximum-bound principle in the proposed scheme, which dissipates the original discrete Ginzburg-Landau energy without any restriction on the time step size. The analysis remains valid when the mobility vanishes at the pure phases, and the discrete energy law further reveals the associated numerical dissipation mechanisms. Numerical experiments confirmed the expected finite element accuracy and verified the maximum-bound and energy-dissipation properties. These results provide a simple, robust, structure-preserving finite element framework for Allen-Cahn dynamics with degenerate mobility.

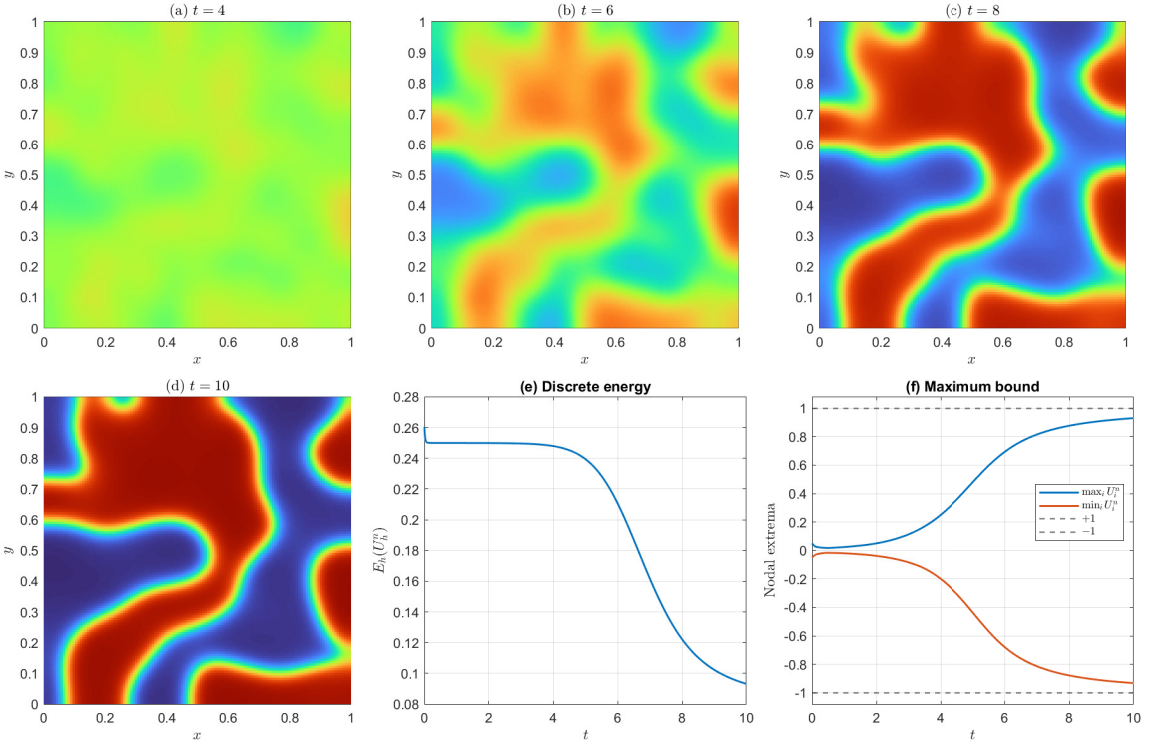


Figure 1: Numerical results for Example 2 with $M(u) = 1 - u^2$, $\varepsilon = 0.02$, $h = 1/128$, and $\tau = 10^{-2}$. Panels (a)–(d) show U_h^n at $t = 4, 6, 8$, and 10, respectively. Panel (e) shows the monotone decay of the discrete energy $E_h(U_h^n)$, while panel (f) confirms that the nodal extrema remain in $[-1, 1]$, which is in agreement with Theorems 3.2 and 3.3.

References

[1] S. M. Allen, J. W. Cahn, A microscopic theory for antiphase boundary motion and its application to antiphase domain coarsening, Acta Metall. 27 (1979), 1085–1095.

[2] J. W. Barrett, J. F. Blowey, Finite element approximation of a degenerate Allen-Cahn/Cahn-Hilliard system, SIAM J. Numer. Anal. 39 (2001), 1598–1624.

[3] Z. Du, T. Hou, A linear second-order maximum-bound principle preserving finite difference scheme for the generalized Allen-Cahn equation, Appl. Math. Lett. 158 (2024), 109250.

[4] D. J. Eyre, Unconditionally gradient stable time marching the Cahn-Hilliard equation, Mater. Res. Soc. Sympos. Proc. 529 (1998), 39–46.

[5] X. Feng, A. Prohl, Numerical analysis of the Allen-Cahn equation and approximation for mean curvature flows, Numer. Math. 94 (2003), 33–65.

[6] H. Fu, D. Hou, Z. Qiao, B. Zhang, Dynamic-stabilization-based linear schemes for the Allen-Cahn equation with degenerate mobility, J. Comput. Math. 44 (2026), 1219–1247.

[7] D. Hou, L. Ju, Z. Qiao, A linear second-order maximum-bound principle-preserving BDF scheme for the Allen-Cahn equation with a general mobility, Math. Comp. 92 (2023), 2515–2542.

[8] D. Hou, T. Zhang, H. Zhu, A linear second order unconditionally maximum-bound principle-preserving scheme for the Allen-Cahn equation with general mobility, Appl. Numer. Math. 207 (2025), 222–243.

[9] D. Hou, H. Liu, L. Ju, Unconditionally original energy-dissipative and MBP-preserving Crank-Nicolson scheme for the Allen-Cahn equation with general mobility, Comput. Math. Appl. 191 (2025), 86–104.

[10] X. Li, W. Huang, Maximum principle for the finite element solution of time-dependent anisotropic diffusion problems, Numer. Meth. Part. Diff. Eqs. 29 (2013), 1963–1985.

[11] C. Li, Y. Huang, N. Yi, An unconditionally energy stable second order finite element method for solving the Allen-Cahn equation, J. Comput. Appl. Math. 353 (2019), 38–48.

[12] J. Shen, T. Tang, J. Yang, On the maximum principle preserving schemes for the generalized Allen-Cahn equation, Commun. Math. Sci. 14 (2016), 1517–1534.

[13] X. Xiao, R. He, X. Feng, Unconditionally maximum principle preserving finite element schemes for the surface Allen-Cahn type equations, Numer. Meth. Part. Diff. Eqs. 36 (2020), 418–438.

[14] J. Yang, N. Yi, H. Zhang, High-order, unconditionally maximum-principle preserving finite element method for the Allen-Cahn equation, Appl. Numer. Math. 188 (2023), 42–61.